Growth and Orientation of Naphthalene Films on Ag(111)

W. X. Huang[†] and J. M. White*

Department of Chemistry and Biochemistry, Center for Materials Chemistry, The University of Texas at Austin, Austin, Texas 78712

Received: December 12, 2003; In Final Form: February 24, 2004

The growth of naphthalene films on Ag(111) was studied by reflection absorption infrared spectroscopy (RAIRS) and temperature-programmed desorption (TPD). The molecular orientation of naphthalene was also calculated using the surface infrared spectroscopy selection rule. Naphthalene adsorption at 210 K is limited to a monolayer. During dosing at 150 K, naphthalene forms a metastable second layer prior to multilayer formation. TPD results suggest that the metastable second layer desorbs at a temperature about 9 K lower than the multilayer and that the second layer rearranges to become part of the multilayer as the latter forms. RAIRS results indicate that naphthalene rings in the monolayer lie parallel to the surface, whereas in the metastable layer these rings are tilted away from the surface plane.

1. Introduction

The interaction of organic molecules with metals and the growth of corresponding thin films are receiving more and more attention because of practical implications in surface and materials science, such as the creation of organic thin film semiconductor devices[1] and nanotribology.[2] Recent advances in molecule-based electronic and optoelectronic devices have inspired the need for a fundamental understanding of the structure and growth of thin molecular films.

Two key issues are usually addressed regarding the growth of thin molecular films. The first is the mode of growth. Similar to the growth of atomic solid films, the deposition of molecular solids follows three main growth modes: layer-by-layer, formation of three-dimensional crystallites, and monolayer deposition followed by clustering. In general, the growth mode is determined by competition between molecule−substrate and intramolecular interactions. The second key issue is adsorbate orientation. Because molecule−molecule and molecule−substrate forces can be highly anisotropic, orientational transitions are expected during deposition of molecular solids. Particularly at an interface between differing materials, the molecular orientation is expected to influence the optical and electronic properties of the resulting combined structure.

Benzene has been employed as a probe to study the effects of anisotropic molecule−molecule and molecule−substrate interactions on the growth of molecular thin films. On most metal single-crystal surfaces, for example, Ru(001),[3,4] Ni(100),[5,6] Ni(111),[7] Ni(110),[8] and Mo(110),[9] benzene films, deposited under ultrahigh vacuum (UHV) conditions, appear to go through a metastable structure as the coverage increases from the chemisorbed and physisorbed layers to the bulklike structure. The metastable state desorbs at temperatures 10−15 K below bulk multilayers. One exception is benzene deposited on Cu(111) where a second layer structure, more stable than bulk, forms prior to multilayer formation.[10] Average orientations of benzene within deposited films were derived from high-resolution electron energy loss spectroscopy (HREELS) on Ru(001)[3] and near edge X-ray absorption fine structure (NEXAFS) on Cu(111).[10] The plane of the benzene ring lies parallel to the surface for the chemisorbed or physisorbed layer but is approximately perpendicular to the surface for the metastable layer and the stable second layer.

Recently, the thin film growth of pyridine and aniline on Ag(111) was studied by means of TPD for comparison with benzene.[11] Different mechanisms were observed for thin film growth from the first chemisorbed layer to the bulk structure: aniline grew through thermodynamically stable layered structures, whereas pyridine grew through metastable phases.[11]

In this paper we employed temperature-programmed desorption (TPD) and reflection absorption infrared spectroscopy (RAIRS) to study the growth of naphthalene thin films on Ag(111), and evidence was found to support the formation of a metastable second layer structure. TPD results show that the second layer naphthalene desorbs at a temperature 9 K lower than naphthalene multilayers. RAIRS results indicate that the rings of naphthalene in the first layer lie parallel to the surface, whereas the second naphthalene layer adsorbs in an orientation with the molecular plane significantly tilted away from the surface.

2. Experimental Section

Experiments were performed in a two-level ultrahigh vacuum chamber with a base pressure of $1.0-2.0 \times 10^{-10}$ Torr.[12] The upper level was equipped with a Nicolet Magna-IR 860 spectrometer for RAIRS, a SRS RGA 200 for residual gas analysis, and an ion sputtering gun. The lower level was comprised of a UTI-100C mass analyzer for TPD and a single-pass cylindrical mirror analyzer for Auger electron spectroscopy (AES).

The Ag(111) sample was mounted on a tungsten loop attached to electrically isolated copper bars that were thermally connected to a hollow copper block filled with liquid nitrogen. The sample temperature was measured by a type K thermocouple inserted into the edge of the crystal and was controlled between 77 and 920 K with a commercial temperature controller. The Ag(111)

* Corresponding author. E-mail: jmwhite@mail.utexas.edu. Fax: (512) 471−9495.

[†] Present address: Fritz-Haber-Institut der Max-Planck-Gesellschaft, Berlin 14195, Germany.

10.1021/jp0378384 CCC: $27.50
Published on Web 03/30/2004

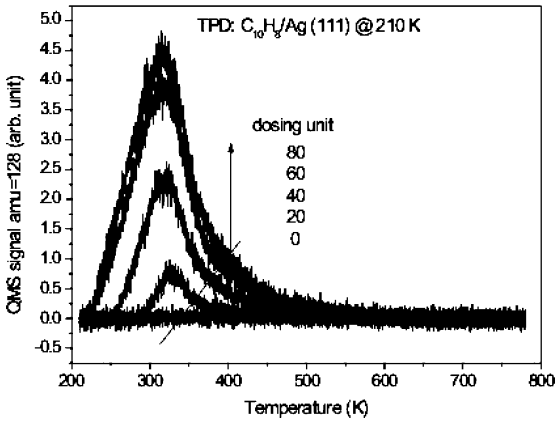

Figure 1. TD spectra following naphthalene doses on Ag(111) at 210 K.

surface was cleaned by repeated cycles of sputtering and annealing until no contaminants could be detected by AES.

Naphthalene deposition was accomplished using a pinhole doser, the end of which terminated 2 mm from the crystal surface during dosing. After dosing, the doser was retracted 25 mm. During experiments, the parts through which naphthalene traveled were kept at constant temperatures of 440 and 350 K, inside and outside the UHV chamber, respectively. Naphthalene was degassed before using and the purity was verified by RGA. To dose, 0.01 Torr of naphthalene vapor was added to a source vessel that was separately connected to the pinhole doser and a turbomolecular pump (TMP) by two VCR valves (closed). The dosing was initiated by opening the valve between the vessel and the doser and terminated by opening the valve between the vessel and the TMP to evacuate the naphthalene vapor in the vessel. The naphthalene exposures (dose unit) are reported as the product of naphthalene vapor pressure in the source vessel (0.01 Torr) × dosing time (min) × 1000.

RAIRS spectra, taken with a mercury−cadmium−telluride (MCT) detector, were collected by summing 1000 scans at 4 cm^{-1} resolution between 650 and 4000 cm^{-1}. The total collection time was about 10 min. TPD spectra were collected at a ramp rate of 1.5 K/s.

In the current instrument design, the sample position for RAIRS experiments is the same as that for dosing. Because of the relatively low pumping speed of the turbomolecular pump (TMP) for naphthalene, during the collection of RAIRS spectra (∼10 min), variable amounts of naphthalene continued to be dosed even though the doser is off. This resulted in a discrepancy when comparing surface coverages estimated using TPD with those from RAIRS. To test this, we compared pairs of TPD spectra, one taken immediately after dosing and the other after a time delay in the dose−RAIRS position. The latter TPD area was larger by a fractional amount that decreases with larger doses.

3. Results

3.1. Naphthalene Dosed at 210 K. When dosed at 210 K, the TPD spectra of naphthalene (Figure 1) shows a single saturable desorption peak, indicating that a monolayer, but not multilayers, forms. AES after successive TPD experiments detected no accumulation of carbon on the surface, implying that naphthalene adsorbs molecularly and does not dissociate upon heating. At low coverage, the naphthalene desorption peak centers at 325 K. It broadens and shifts to lower temperatures with the increasing coverage. The shift to lower temperature is attributed to the repulsive interactions between adsorbed

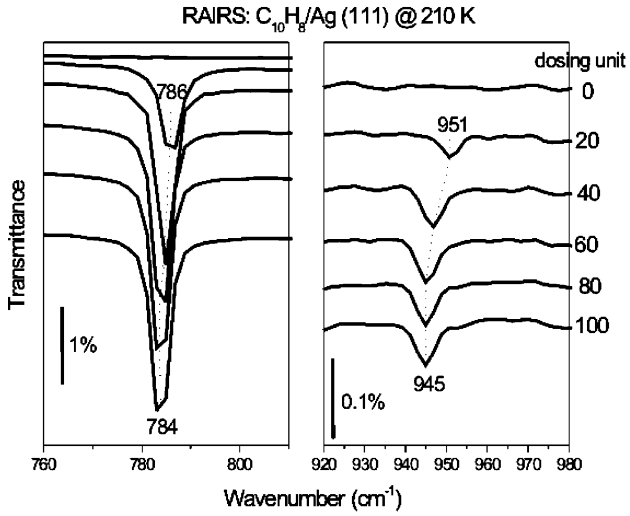

Figure 2. RAIRS spectra following naphthalene doses on Ag(111) at 210 K.

molecules within the monolayer. This behavior is similar to that of other aromatic molecules on noble metal surfaces,[7,10,13] including $C_{10}H_8$ on Cu(111).[13]

Figure 2 shows RAIRS spectra of naphthalene on Ag(111) dosed at 210 K where multilayers do not form. Only two vibration peaks, 786 and 951 cm^{-1}, were observed. Both slightly red-shift with increasing coverage, and saturation is evident for doses larger than 60 units. As in TPD, the red shift is attributed to increased repulsive interactions as the coverage grows. By comparison with the IR spectrum of gas phase naphthalene,[14] we assign the peaks at 786 and 951 cm^{-1} to γ_2 and γ_1 C−H bending vibrations of adsorbed naphthalene (the notation in Table 1 is taken from ref 14). We note that both of the observed bands are assigned to out-of-plane vibrations, and these modes have transition dipole moments that are oriented perpendicular to the molecular plane of naphthalene.

Making use of the so-called RAIRS selection rule,[15] the average orientation of molecules adsorbed on metals can be derived through symmetry analysis of the observed RAIRS bands. A vibrational mode will not be active unless there is a nonzero projection of the transition dipole moment along the surface normal.[15] Applying this rule, the presence of only two vibrational modes, both out-of-plane, for monolayer naphthalene clearly, and not unexpectedly, indicates that the plane of the rings of the first layer of naphthalene molecules lies parallel to the Ag(111) surface. We designate this orientation as *flat*. The same orientation is found from spectroscopic data for other aromatic molecules adsorbed on Ag(111),[16] Ru(001),[3] and Cu-(111).[10] Recent microscopy (STM) results gave direct, spatially resolved evidence showing that monolayer benzene, naphthalene, naphthoquiones, and anthracene lie flat on Cu(111), Rh-(111), and Pt(111).[17,18]

Figure 3 compares the naphthalene coverage estimated from TPD (the integrated area of the thermal desorption peak) and from RAIRS (the integrated area of the peak between 770 and 810 cm^{-1}). The thermal desorption peak area increases linearly with increasing dose and is saturated after dosing more than 80 units of naphthalene; however, the RAIRS peak intensity saturates after dosing 40 units of naphthalene. As noted above, we attribute this discrepancy to the continued slow dosing of naphthalene onto Ag(111) during the course of collecting RAIRS spectra because of the instrumental design and the low pumping speed for naphthalene.

TABLE 1: Assignment of Observed IR Bands for $C_{10}H_8$ Adsorption on Ag(111) at 150 K

			vibrational frequency (cm^{-1})			
				$C_{10}H_8$/Ag(111)		
	symmetry	vibrational modes [a]	$C_{10}H_8$ (from ref 14) [b]	monolayer	metastable layer	multilayer
out-of-plane	B_{3u}	γ_{C-H}	780 g	786	781	792
	B_{3u}	γ_{C-H}	955 g	952	942	960
	B_{2g}	γ_{C-H}	875 av			847
	B_{2g}	γ_{C-H}	983 sd			981
in-plane	B_{2u}	ν_{C-C}	1008 g		1007	1007
	B_{1u}	β_{C-H}	1125 g		1124	1124
	A_g	b_{C-H}	1144 sd			1142
	B_{1u}	β_{C-H}	1265 g		1268	1276
	B_{2u}	β_{C-H}	1389 g		1390	1390
	B_{1u}	ν_{C-C}	1595 g		1595	1595
	B_{1u}	ν_{C-H}	3058 g		3056	3056

[a] γ = out-of-plane bend; β = in-plane bend; ν = stretch. [b] g = gas value; sd = solid value; av = a phase-averaged value.

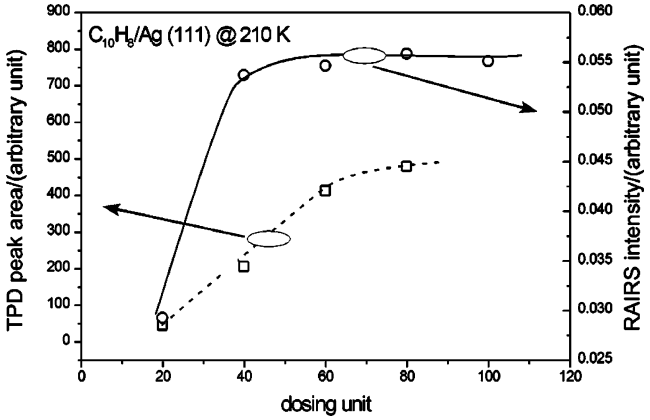

Figure 3. Comparison of the amounts of naphthalene on Ag(111) based on TPD and RAIRS results at 210 K.

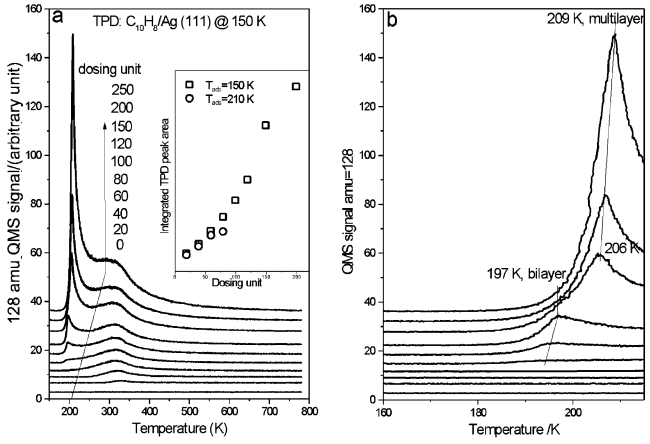

Figure 4. (a) TPD spectra following naphthalene doses on Ag(111) at 150 K. The amount of naphthalene desorbing from the surface is plotted as a function of dose in the inset. (b) Low-temperature region of the TPD spectra of Figure 4a.

3.2. Naphthalene Dosed at 150 K. *3.2.1. TPD Results.* Upon lowering the dosing temperature from 210 to 150 K, the TPD spectra change. There are as many as three local maxima (Figure 4a). As expected, low doses lead to one peak in TPD that is attributed to monolayer desorption. This peak, initially centered at 330 K, shifts to lower temperature with increasing coverage. The second peak, near 194 K, appears after dosing 80 units of naphthalene. This maxima shifts to higher temperatures when the dose is increased, implying the existence of attractive interactions within adsorbed naphthalene molecules. The third desorption peak is present for doses of 150 units or more. This peak, however, appears at a higher desorption temperature (206 K) than the second peak, shifts higher with increasing coverage, and does not saturate with the increased dosing. These are characteristic of zero-order multilayer desorption, and thus, this third peak is attributed to desorption from a bulk solid film of naphthalene.

By magnifying the low-temperature part of the desorption traces in Figure 4a, the second and third peaks can be clearly distinguished based on their distinctly different leading edges (Figure 4b). Two interesting features of the second desorption peak are found: (1) although it appears earlier in the TPD spectra, the second peak desorbs at a temperature about 9 K lower than the multilayer, and (2) the second desorption peak attenuates as the multilayer coverage increases and completely vanishes for large doses, that is, the second desorption peak is quenched after the formation of the multilayer. These TPD features resemble those of a metastable layer of benzene desorbing from Ru(001).[3,4] Thus, we propose that the second desorption peak results from a metastable second layer of naphthalene that rearranges when thicker layers, that is, bulklike multilayers, begin to form.

The inset in Figure 4a plots the integrated TPD peak area as a function of dose units. For low doses, the area increases linearly, and the data for doses at 150 K coincide with those for doses at 210 K. This confirms that the pinhole doser is reproducible. Peak areas for large doses at 150 K rise supralinearly for, as yet, unknown reasons. Possibilities include one or both of the following: an increased sticking coefficient when the multilayer region is accessed and a relatively low pumping speed for naphthalene. A contribution from the latter is indicated by the long tail, especially for large doses.

3.2.2. RAIRS Results. Figure 5 presents the RAIRS results when naphthalene was dosed at 150 K. Up to 40 dose units, the spectra are the same as those for naphthalene dosed at 210 K, that is, out-of-plane C−H bending modes at 786 and 951 cm^{-1}. Thus, we conclude that dropping the dose temperature from 210 to 150 K does not lead to a different orientation of the monolayer; in both cases, monolayer naphthalene adsorbs with its molecular plane parallel with the Ag(111) surface.

For doses exceeding the monolayer, additional bands appear. Detailed inspection reveals that between 60 and 120 dose units, six new bands are observed—1007, 1124, 1268, 1390, 1595, and 3056 cm^{-1}. When the naphthalene dosing exceeds 150 dose units, five additional bands appear—792, 847, 960, 981, and 1142 cm^{-1}. On the basis of comparison with the IR spectrum of gas phase naphthalene,[14] most of these additional bands can be ascribed to *in-plane* vibrations (Table 1). On the basis of

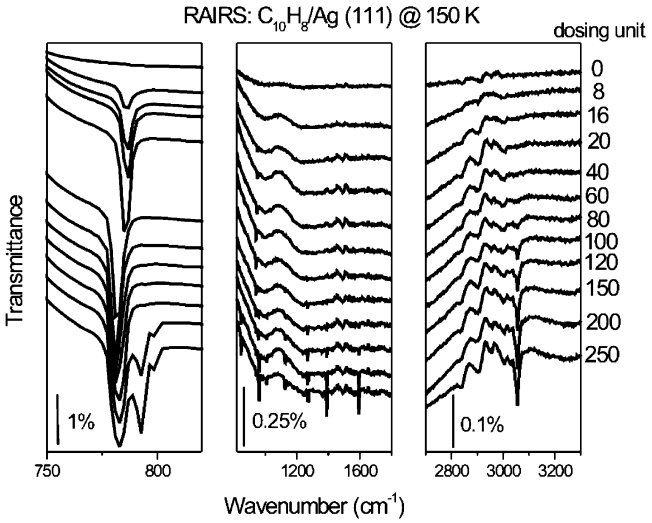

Figure 5. RAIRS spectra following naphthalene doses on Ag(111) at 150 K.

the surface infrared selection rule,[15] the appearance of in-plane vibrational modes at large doses indicates that the orientation of the plane of the naphthalene rings tilts away from the Ag-(111) surface, at least for molecules that are not in the first layer.

4. Analyzing Growth Modes

The growth mode of atomic solid films on well-defined surfaces has often been discussed in terms of an Auger signal versus deposition time plot during the course of thin film growth.[19] Because molecular thin films are vulnerable to electron-induced destruction, this method is of limited value in the present case. To assess growth for the first few layers, we correlate the peak intensity of a selected vibrational band (RAIRS) versus dose unit.

The integrated area A_i of infrared band i can be written as[20]

$$A_i = \frac{32\pi^3 n}{hc\alpha} M_{iz}{}^2 \nu_{io} G(\theta) \qquad (1)$$

where M_{iz} is the transition dipole moment component in the direction of the surface normal, n is the number of dipoles (number of molecules), α is the surface area, ν_{io} is the resonant frequency, and $G(\theta)$ is a function which is dependent upon the angle of incidence and the dielectric constant of the substrate. α, ν_{io} and $G(\theta)$ do not depend on the adsorbed molecule.

Assuming the IR band intensity from a few layers (j) of molecules involves insignificant screening effects, we sum over layers to obtain

$$A_i = \frac{32\pi^3}{hc\alpha} \nu_{io} G(\theta) \sum_j M_{iz}(j)^2 n(j) \qquad (2)$$

Allowing M_{iz} to vary from layer to layer, but not within a given layer, we differentiate eq 2 to form

$$\mathrm{d}A_i = \sum_j M_{iz}(j)^2 \, \mathrm{d}n(j) \qquad (3)$$

Different predictions follow depending on subsidiary assumptions made about $M_{iz}(j)$.

(1) If M_{iz} is constant for all layers A_i will vary linearly with $n(j)$ and no conclusion can be made concerning the growth mode.

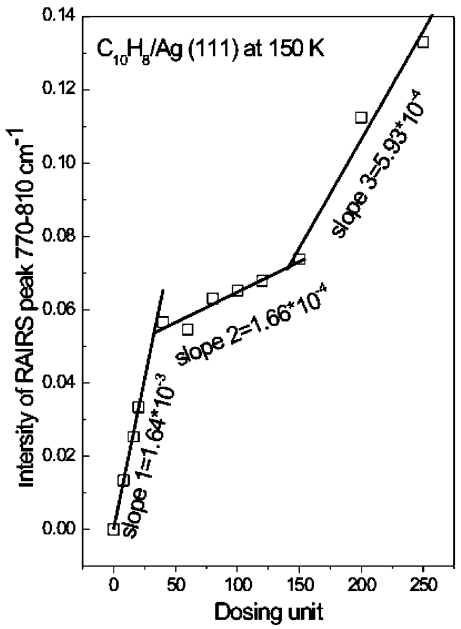

Figure 6. Integrated area of the γ_{C-H} vibrational band (770−810 cm^{-1}) of naphthalene on Ag(111) at 150 K as a function of dose.

(2) If M_{iz} changes with j, different growth modes can be distinguished: (a) For layer-by-layer (Franck−van der Merwe) growth, A_i will comprise a series of linear segments with a slope change in passing from one layer to the next. (b) For 3D island (Volmer−Weber) growth, A_i will have no linear regions longer than a small fraction of the first layer. (c) If the first layer forms and is followed by 3D island growth, Stranski−Krastanov **(**SK) mode, A_i increases linearly for the first layer but then follows a nonlinear profile for all higher doses.

5. Discussion

5.1. Growth of Naphthalene on Ag(111) at 150 K. In our experiments, we chose the most intense vibrational band of adsorbed naphthalene (γ_2 out-of-plane C−H bending vibration at 785 cm^{-1}) and plotted the integrated peak area A_i versus dose units (Figure 6). The data are adequately fit by three linear segments with changes of slope at 32 and 140 dose units. When the extra coverage accumulated during RAIRS is accounted for, similar results were obtained when plotting A_i versus the integrated peak area of the corresponding TPD spectra (not shown). We conclude that the first and the second linear segments, respectively, correspond to the growth of the monolayer and metastable layer of naphthalene on Ag(111) and that the slope change at 32 dose units indicates the completion of the monolayer growth. The second slope change at 140 dose units indicates completion of the metastable layer growth and the beginning of multilayer growth. The third linear section corresponds to the multilayer growth. Although additional results are needed to prove it, we suppose the linear relationship between A_i and dose unit in the multilayer is the result of the average $M_{iz}(j)$ being constant for $j > 2$, that is, case (1) of section 4.

The stability of the metastable layer as the multilayer forms is an important issue. The thermal desorption results show that the TPD peak of the metastable layer is suppressed as the multilayer forms (150 dose unit) and finally vanishes (250 dose unit). The suppression is attributed to the conversion of the metastable layer into the multilayer for thick layers. However, TPD cannot determine whether the conversion occurs during adsorption or during heating. RAIRS helps clarify this issue.

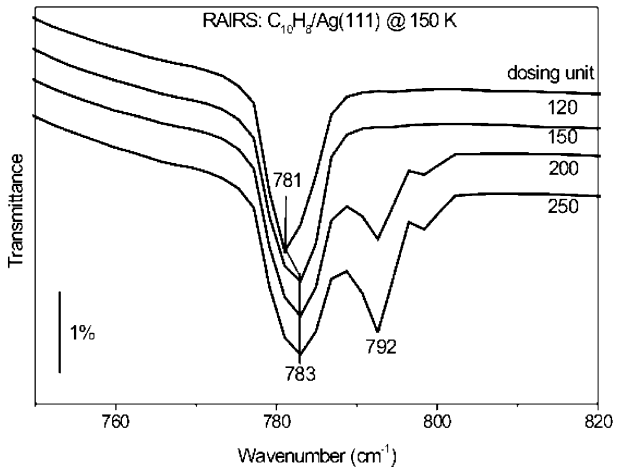

Figure 7. The γ_{C-H} vibrational band of naphthalene on Ag(111) at 150 K for four doses between 120 and 250 units.

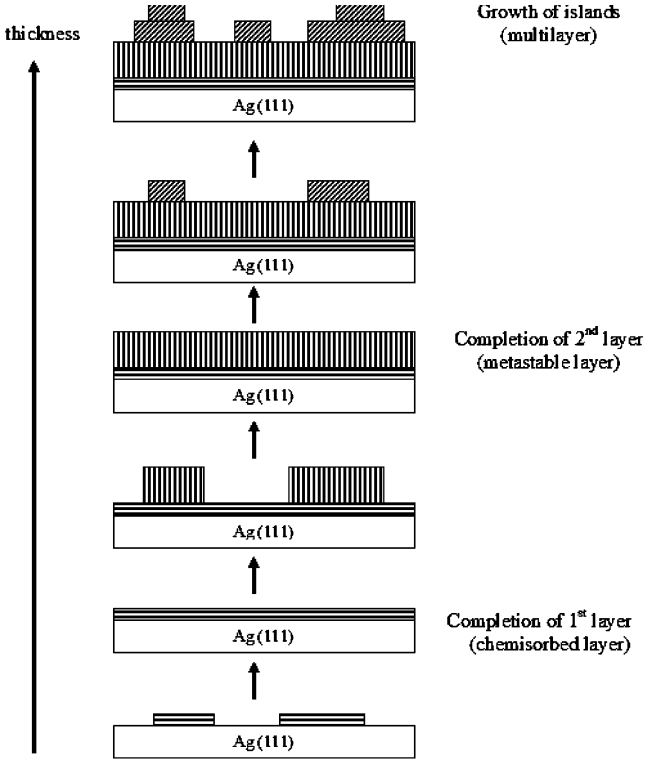

Figure 8. Schematic of the proposed Stranski−Krastanov (SK) growth of naphthalene on Ag(111) at 150 K.

Figure 7 compares the γ_2 out-of-plane C−H bending vibration mode of naphthalene for doses from 120 to 250 units. The γ_2 peak (781 cm^{-1}) of the monolayer and of the metastable layer blue-shift (∼2 cm^{-1}) and slightly intensify when the dose increases from 120 (monolayer + metastable layer) to 150 units (monolayer + metastable layer + multilayer). Above 150 dose units, there is no additional shift or intensification but a new band appears at 792 cm^{-1}, assigned to the γ_2 vibration of the multilayer. The results indicate that the underlying monolayer and metastable layer remain intact at 150 K and multilayer is added up to 250 dose units, that is, 8× the dose defined as 1 ML (1 ML corresponding to 32 dose units on the basis of Figure 6).[21] From this we conclude that the conversion of the metastable layer into multilayer is thermally activated and occurs during the course of heating.

To sum up, Figure 8 sketches the proposed growth process based on the A_i versus dose plot (Figure 6). We conclude that the growth of naphthalene on Ag(111) follows Stranski−Krastanov type growth: a first layer and a metastable layer are completed before 3D multilayer islands form.

5.2. Orientation of Naphthalene Thin Films on Ag(111). According to eq 3, the slopes of A_i versus dose reflect the value of M_{iz}^2. In terms of M_i, the total transition dipole moment, the normal component, M_{iz}, can be written

$$M_{iz} = M_i \cos\theta \tag{4}$$

where θ is the angle between M_i and the surface normal. The ratio of the monolayer slope to the metastable layer slope is

$$\frac{\text{slope1}}{\text{slope2}} = \frac{M_{iz}(1)^2}{M_{iz}(2)^2} = \left(\frac{M_i(1)\cos\theta_1}{M_i(2)\cos\theta_2}\right)^2 \tag{5}$$

For weakly adsorbed molecular films, the transition dipole moment is only slightly altered by the substrate, and M_i will not change significantly from layer to layer. Thus,

$$\frac{\text{slope1}}{\text{slope2}} = \left(\frac{\cos\theta_1}{\cos\theta_2}\right)^2 \tag{6}$$

The angle between M_i and the molecular plane can be easily obtained through symmetrical analysis, and thus, we can acquire the molecular orientation in different layers.

In the present study, we chose the γ_2 out-of-plane C−H bending vibration mode of naphthalene to plot the A_i versus dose curves. For this mode, the transition dipole moment M_i is perpendicular to the molecular plane, that is, the angle between M_i and the surface normal is the same as the angle between the molecular plane and the Ag(111) surface. Because the molecular plane is parallel to the surface for monolayer naphthalene ($\theta_1 = 0°$), eq 6 can be solved for θ_2 using the slopes from Figure 6. The result, $\theta_2 = 71.5°$, indicates that the metastable layer bonds with its ring structure far from parallel to the surface. Although the average orientation of the 3D multilayer structure remains to be determined, one clear conclusion that can be drawn is that the ensemble average multilayer orientation of the plane of naphthalene lies at an intermediate angle. These orientations of naphthalene on Ag(111) are qualitatively consistent with those for benzene on Ru(001) and Cu(111).[3,4,10]

5.3. Populations of Naphthalene in the Metastable Layer. Because the planes of naphthalene molecules in the monolayer lie parallel to the Ag(111) surface whereas those in the metastable layer tilt on average 71.5° away from the surface, it is likely that the real number density in the saturated metastable layer is larger than in the saturated monolayer. Based on dose unit ratio of 4.3 (directly from Figure 6), we conclude that naphthalene population in the metastable layer is about as 3 times that in the monolayer.

For C_6H_6 adsorption on Ru(001), the population of the metastable layer is at least 1.3 times that of the physisorbed layer.[3] For C_6H_6 on Cu(111), a stable second layer is formed, and the ratio of the benzene population of the stable second layer to that of the underlying chemisorbed layer is 1.8 based on TPD peak areas.[10] Considering the larger aspect ratio of naphthalene compared to benzene, the value of 3 is reasonable for the ratio the naphthalene population of the metastable layer to that of the underlying chemisorbed monolayer.

5.4. Comparison to Other Work. The growth mode of molecular thin films is determined by the molecule−substrate and molecule−molecule interactions. Previous studies of benzene film growth show that the first layer of benzene lies flat

on the substrate to maximize the molecule−substrate interaction and subsequent growth strongly depends on the substrate. On inactive graphite, subsequent deposition results in the formation of bulk benzene crystallites.[22] On active metal surfaces, such as Ru(001),[3,4] Ni(100),[5,6] Ni(111),[7] Ni(110),[8] and Mo(110),[9] benzene deposition beyond the first layer involves the formation of a physisorbed layer with its molecular plane parallel to the plane of the chemisorbed benzene. This is followed by a metastable layer with the C_6H_6 planes oriented perpendicular to the underlying physisorbed layer. Subsequent growth forms the bulk molecular crystal structure. On less active metal surfaces such as Cu(111), benzene deposition leads to the formation of a stable second layer that is perpendicular to the underlying chemisorbed layer prior to the growth of multilayers.

Few studies have examined the growth of aromatic molecules other than benzene on metal surfaces. Similar to benzene on Cu(111), TPD results indicate that naphthalene forms a stable second layer between the chemisorbed layer and the multilayer on Cu(111) for doses at 165 K.[13] The present study clearly shows that for naphthalene deposition on Ag(111) at 150 K, the plane of the ring is parallel to the substrate surface in the first layer, nearly perpendicular to it in a metastable second layer, and an average orientation between these limits in the subsequently formed multilayer.

Taking previous and present results together, the growth of anaromatic molecular film on metal surfaces typically involves a transition layer between a chemisorbed monolayer (and the following physisorbed layer in case of active metal surfaces) and a bulklike multilayer. Prior to the transition layer, the molecule−substrate interaction prevails and the molecular film grows layer-by-layer following an orientation that maximizes the molecule−substrate interaction; after the transition layer, the molecule−molecule interaction prevails and the film takes on the bulk molecular crystal structure, often in 3D island form. Anisotropic molecule−molecule interactions likely determine the orientation of the transition layer. In the case of benzene, the transition layer molecular planes are perpendicular to the underlying layer planes.[23] The first and second layers of naphthalene on Ag(111) behave in much the same way.

Comparing naphthalene adsorption on Ag(111) and Cu(111), we infer that the thermal stability of the transition layer compared with the multilayer is related to the molecule−substrate interaction; the transition layer is more stable than the multilayer on Cu(111)[13] but is less stable on Ag(111). The interaction between naphthalene molecules in the transition layer and the multilayer should be nearly the same on these two surfaces. The difference between their stability must originate from the substrate and likely reflects the general observation that Cu(111) is slightly more chemically active than Ag(111) in gas−surface processes.

6. Conclusions

Naphthalene deposition on Ag(111) at 210 K forms a saturable monolayer, but no multilayer, and the molecular planes lie parallel to the substrate surface. At 150 K, multilayer growth occurs and exhibits a Stranski−Krastanov behavior. Three distinct regimes have been identified: monolayer, metastable layer, and multilayer. In the monolayer, the naphthalene molecules bond with the plane of their rings parallel to the surface. The metastable layer desorbs at a temperature about 9 K lower than the multilayer and is oriented with the molecular plane tilted more than 70° away from parallel to the surface. The multilayer grows with an average tilt angle that lies below 70°.

Acknowledgment. The work is supported by the National Science Foundation (CHE0070122), the Robert A. Welch Foundation, and the Center for Materials Chemistry of the University of Texas. Fruitful discussions with Wei Wei are gratefully acknowledged.

References and Notes

(1) Forrest, S. R. *Chem. Rev.* **1997**, *97*, 1793.
(2) In *Handbook of Micro/nano Technology*, 2nd ed.; Bhushan, B., Ed.; CRC Press: Boca Raton, FL, 1999.
(3) Jakob, P.; Menzel, D. *Surf. Sci.* **1989**, *220*, 70.
(4) Jakob, P.; Menzel, D. *J. Chem. Phys.* **1996**, *105*, 3838.
(5) Blass, P. M.; Akhter, S.; White, J. M. *Surf. Sci.* **1987**, *191*, 406.
(6) Myers, A. K.; Benziger, J. B. *Langmuir* **1987**, *3*, 414.
(7) Steinruck, H. P.; Huber, W.; Pache, T.; Menzel, D. *Surf. Sci.* **1989**, *218*, 293; **1987**, *217*, 103.
(8) Huntley, D. R.; Jordan, S. L.; Grimm, F. A. *J. Phys. Chem.* **1992**, *96*, 1409.
(9) Liu, A. C.; Friend, C. M. *J. Chem. Phys.* **1988**, *89*, 4396.
(10) Xi, M.; Yang, M. X.; Jo, S. K.; Bent, B. E.; Stevens, P. *J. Chem. Phys.* **1994**, *101*, 9122.
(11) Yang, C. T.; Rockey, T. J.; Pursell, D.; Dai, H. L. *J. Phys. Chem.* **2001**, *105*, 11945.
(12) Huang, W. X.; White, J. M. *Surf. Sci.* **2002**, *513*, 399.
(13) Wang, H. F.; Dutton, G.; Zhu, X. Y. *J. Phys. Chem. B* **2000**, *104*, 10332.
(14) Sellers, H.; Pulay, P.; Boggs, J. E. *J. Am. Chem. Soc.* **1985**, *107*, 6487.
(15) Chabal, Y. J. *Surf. Sci. Rep.* **1988**, *8*, 214.
(16) Yannoulis, P.; Dudde, R.; Frank, K. H.; Koch, E. E. *Surf. Sci.* **1987**, *189/190*, 519.
(17) Wan, L. J.; Itaya, K. *Langmuir* **1997**, *13*, 7173.
(18) Yau, S. L.; Kim, Y. G.; Itaya, K. *J. Phys. Chem. B* **1997**, *101*, 3547.
(19) Argil, C.; Rhead, G. E. *Surf. Sci. Rep.* **1989**, *10*, 277.
(20) Persson, B. N. *J. Solid State Commun.* **1979**, *30*, 163.
(21) Inferred from the TPD spectra shown in Figure 4, 1 ML corresponds to a dosing between 60 and 80 dose units. The discrepancy (about 40 dosing units) between the definitions of 1 ML from TPD results and from RAIRS results is due to the continuing dosing of naphthalene on the surface during the course of RAIRS collection after the dosing is off, as mentioned in the Experimental Section and section 3.1.
(22) Cameson, I.; Rayment, T. *Chem. Phys. Lett.* **1986**, *123*, 150.
(23) Craven, C. J.; Hatton, P. D.; Howard, C. J.; Pawley, C. S. *J. Chem. Phys.* **1993**, *98*, 8236.